



Monodromy of the LiNC/NCLi molecule

M. Joyeux ^a, D.A. Sadovskii ^{b,*}, J. Tennyson ^c

^a *Laboratoire de Spectrométrie Physique, Université Joseph Fourier – Grenoble I, UMR 5588 du CNRS, Boîte Postale 87, St. Martin d'Hères 38 402, France*

^b *Physique Department, Université du Littoral, MREID, 145 av M. Schumann, Dunkerque 59 140, France*

^c *Department of Physics and Astronomy, University College London, Gower Street, London WC1E 6BT, UK*

Received 2 October 2003; in final form 23 October 2003

Abstract

Using the potential surface of Essers, Tennyson, and Wormer in [Chem. Phys. Lett. 89 (1982) 223], we show that the system of bending vibrational states of the isomerizing molecule LiNC/NCLi has monodromy. On the basis of a deformed spherical pendulum model, we explain dynamical and geometric reasons of this phenomenon and of its absence in the similar system HCN/CNH.

© 2003 Elsevier B.V. All rights reserved.

Monodromy is an interesting property of certain quantum systems whose levels cannot be labeled globally by one set of quantum numbers. More precisely, even though such systems have no obvious subsystems, each with its own set of quantum numbers, quantized energy cannot be expressed as one smooth function of any quantum numbers. Dynamical meaning of this phenomenon can be uncovered [1,2] by analyzing monodromy of the corresponding classical analogue. For the details of the classical theory see [3] and references therein.

Monodromy is not uncommon. It has been found in several fundamental atomic and molecular systems, notably the perturbed hydrogen atom [4], Stark effect in rotating dipolar molecules [5], rotating quasi-linear triatomic molecules [6], systems with coupled angular momenta [7], and H_2^+ [8]. Floppy triatomic molecules with linear equilibrium configuration(s) form another set of candidate systems with monodromy [9]. In this Letter, we describe monodromy of LiNC/NCLi. We compare this system to HCN/CNH, which we have analyzed recently in [10].

Our study of LiNC/NCLi uses the two-dimensional potential [14] which gives the energy of the LiNC configurations as function of the bending angle γ and Li–NC stretch distance R for the length r of the N–C bond fixed at 2.186 bohr. We assume approximate separability of the two degrees of freedom corresponding to overall

* Corresponding author.

E-mail addresses: marc.joyeux@ujf-grenoble.fr (M. Joyeux), sadovskii@univ-littoral.fr (D.A. Sadovskii), j.tennyson@ucl.ac.uk (J. Tennyson).

rotations of the molecule as a whole and we only consider states without such rotations. For these states the total angular momentum J equals the angular momentum ℓ induced by the rotations of Li about axis N–C. The other bending degree of freedom is described by γ and the remaining third degree is stretching vibrations of R . We find the minimum energy path $R(\gamma)$ and consider small stretching oscillations about this path. There is no prominent low order resonance between these oscillations and the bending mode vibrations. This allows us to average the stretching mode out using the quantum analogue [13] of the canonical perturbation theory [11,12] and to introduce stretching quantum number n_R . We obtain the reduced effective bending mode Hamiltonian $H_{\ell, n_R}(p_\gamma, \gamma)$ and use it for the ground stretching state with $n_R = 0$. We study *all* ℓ -states and the advantage of our approach is that the value of quantum number ℓ is predefined.

Using $H_{\ell, 0}(p_\gamma, \gamma)$ we computed quantum energies for each ℓ . For $\ell = 0$ these energies are in good agreement (typically a few cm^{-1}) with full quantum calculations in [15] for $J = 0$ and this justifies our approach. We also found energies of classical *relative equilibria* [3,5] which correspond to Li rotating about the axis of N–C at constant γ and can be found as equilibria of the classical analogue system with reduced Hamiltonian $H_{\ell, 0}(p_\gamma, \gamma)$ for $\ell \neq 0$. For $\ell = 0$ we have two stable linear equilibria of which LiNC is the lowest in energy, and a barrier separating the two wells.

Results of our computation are presented in the form of the *energy–momentum diagram* in Fig. 1. This diagram should be considered as a two-leaf surface. The leaves are bounded by the energies of the relative equilibria. In Fig. 1, the smaller NCLi leaf and the larger LiNC leaf are shaded white and gray, respectively. The NCLi leaf is closed, while the LiNC leaf is unbounded from above. The NCLi leaf is *glued* along its upper boundary to the LiNC leaf. This latter has therefore a critical ‘cut’ surrounded by regular values of the energy–momentum map.

The energies of quantum states form a *lattice* in each of the leaves. Note that the leaves and their lattices overlap in Fig. 1. As the labels imply, the two leaves represent states localized near the LiNC and NCLi equilibria, but the LiNC leaf also includes delocalized states which correspond to Li making complete tours in γ about NC. While NCLi states are all ‘locked’ in their leaf, there is nothing to separate localized LiNC states from delocalized states at sufficiently high ℓ .

We determine the monodromy of LiNC/NCLi using the *elementary cell* method of Zhilinskii which blends the initial approach in [1,2] and the methods used to describe the defects of crystal lattices. We begin by choosing a nearly square elementary cell of the LiNC lattice at $\ell = 0$ and energy $E \approx 4000 \text{ cm}^{-1}$, i.e., above the singular cut, see Fig. 1. This cell reflects our choice of *local quantum numbers*, it defines neighbour states whose one or both quantum numbers differ from

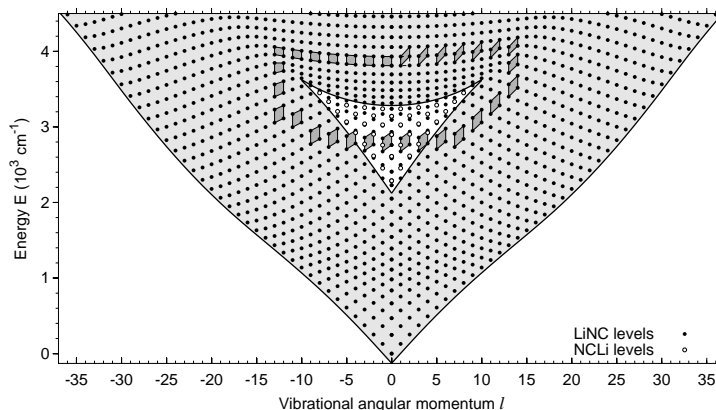


Fig. 1. Energy–momentum diagram of the LiNC/NCLi system computed for the potential in [14]. Filled and hollow circles show levels attributed to the LiNC and NCLi minimums; bold solid lines show energies of classical relative equilibria.

those of the given state by 1. We *continue* our elementary cell along the path which goes counter-clockwise around the cut in *small steps*. Note that in the overlap area of the LiNC and NCLi leaves, we can only use LiNC states (black dots in Fig. 1). At each step the next cell is defined unambiguously by the current cell, i.e., by the current choice of local quantum numbers. However, when we come back to $\ell = 0$ and $E \approx 4000 \text{ cm}^{-1}$ after one tour, the final cell \square does *not* correspond to the original cell \square . The transformation is given by the monodromy matrix $M = \begin{pmatrix} 1 & 1 \\ 0 & 1 \end{pmatrix}$, the monodromy is 1 (the off-diagonal element of M). Note that a very similar phenomenon has been recently studied in [8], where it was somewhat misleadingly called ‘island monodromy’.

The origins of monodromy of LiNC/NCLi can be best understood after comparing the bending motion of LiNC/NCLi to that of the spherical pendulum in [3, Chapter IV.3]. This latter can be represented as a motion of a particle placed in a linear potential $V(z) = z$, e.g., in the field of gravity, and constrained to a sphere. It has one stable equilibrium at the bottom of the sphere that corresponds to the minimum energy and one unstable equilibrium; both equilibria are at $\ell = 0$. In the image of the energy–momentum map, the unstable equilibrium together with all its homoclinic orbits is represented by an isolated critical point, shown by a black circle dot in Fig. 2, left.

Comparing the above to LiNC/NCLi or HCN/CNH, we notice two principal differences: the potential and the ‘shape’. Both linear equilibria of these molecules are stable. This can be described qualitatively if the linear potential of the pendulum is replaced by a quadratic potential $V_c(z) = z - \frac{1}{2}cz^2$. The shape is given by the distance R between Li (or H) and the CN diatom at different values of the bending angle γ along the minimum energy path of the potential surface. In the spherical pendulum R is fixed. As shown in Fig. 3, the molecules have a peanut-like shape because Li (or H) gets closer to the diatom in the T-configuration with $\gamma \approx \frac{1}{2}\pi$. We can model such shape using $R_c(\gamma) = R_{\max}(1 - \epsilon \sin^2 \gamma)$ where $\epsilon \geq 0$ is the *asphericity parameter*.

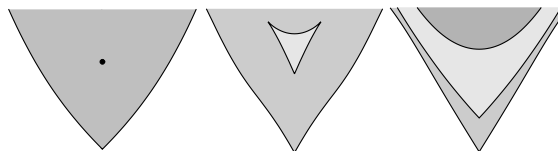


Fig. 2. Energy–momentum values (left to right) of the spherical pendulum [3, Chapter IV.3], LiNC/NCLi (convex), this work, and HCN/CNH (nonconvex) [10].

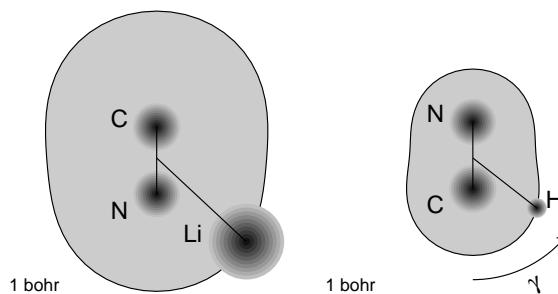


Fig. 3. Geometry of LiNC/NCLi and HCN/CNH; the distance $R(\gamma)$ is computed along the minimum isomerization energy path for the potentials in [14,16], respectively; the size of the atoms is indicated using respective covalent radii.

The energy–momentum ($\mathcal{E}\mathcal{M}$) values in Fig. 2 can be understood qualitatively using the deformed spherical pendulum model with two independent parameters c and ϵ . As explained in detail in [10], the $\mathcal{E}\mathcal{M}$ characteristics of the relative equilibria of this model system are obtained by solving the equations

$$\left\{ F(\gamma) = h, \frac{dF}{d\gamma} = 0 \right\} \quad \text{with}$$

$$F(\gamma) = \ell^2 \left(2mR_c(\gamma)^2 \sin^2 \gamma \right)^{-1} + V_c(\cos \gamma),$$

for (h, ℓ) as functions of $\zeta = \cos \gamma$. These solutions reproduce the $\mathcal{E}\mathcal{M}$ values of the real molecular RE shown by the solid lines in Fig. 2. Note that c and ϵ are the only essential parameters. In particular, c defines the relative energies of the two stable linear equilibria A and B and the barrier X at $\ell = 0$,

$$h_X > h_B > h_A,$$

$$(h_X - h_B)/(h_X - h_A) = (c - 1)^2/(c + 1)^2.$$

Changing the values of R_{\max} and m rescales the ℓ axis, while h can be rescaled and shifted as $\omega h + f_0$ using additional parameters ω and f_0 .

When the deformation of the original system with $c = \epsilon = 0$ is small, i.e., for $c \ll 1$ and $\epsilon \ll 1$, the $\mathcal{E}\mathcal{M}$ diagram does not change qualitatively. When c becomes larger than 1 while $\epsilon \ll 1$, the isolated singular point (Fig. 2, left) becomes a small triangular leaf (Fig. 2, center) glued to the main leaf as we already explained before. When $\epsilon > \frac{1}{3}$ and $c > 1$ this new leaf becomes *unbound* from above at sufficiently high ℓ (Fig. 2, right). At such large ϵ the singular cut, along which the two leaves are glued together, is no longer a finite segment. This cut now separates the $\mathcal{E}\mathcal{M}$ values of the motion localized near the equilibria from those of the delocalized motion. We can no longer loop around the cut in the domain of the regular $\mathcal{E}\mathcal{M}$ values, as we did for LiNC/NCLi (Fig. 1). Consequently, model systems with $\epsilon > \frac{1}{3}$ have no monodromy.

The value of $\epsilon = \frac{1}{3}$ has a remarkably simple geometric meaning. At this value, the shape of the model system bifurcates so that for $\epsilon > \frac{1}{3}$ it develops a ‘waist’. *We conjecture that existence of monodromy in real floppy molecules depends on their convexity.* From the values of R [bohr] 4.35–3.55–4.80 for LiNC/NCLi and 3.18–2.04–2.90 for HCN/CNH, a rough estimate gives respective values of $\epsilon = 0.26$ and $\epsilon = 0.36$. Indeed, while LiNC/NCLi is convex (Fig. 3, left), the HCN/CNH system has a small waist. So the conclusion in [10] that the HCN/CNH molecule has no monodromy (Fig. 2, right) comes as no surprise.

In the present Letter, we have considered *four* of the six internal degrees of freedom of LiNC/NCLi. Of the two stretching vibrations, the NC stretch was frozen a priori in the potential [14], while the oscillation of the Li–NC distance R was averaged out and represented by quantum number n_R . We also included rotation of Li about the axis of the NC diatom. This degree of freedom was represented by the vibrational angular momentum ℓ . And finally, we described explicitly the large amplitude bending motion in γ . We have found that this *subsystem* has monodromy. Before extending our result to the complete LiNC/NCLi system, we should investigate the interaction between the four degrees of freedom we analyzed and

the two remaining degrees related to overall rotations of the molecule. In our treatment based on [11–13] we neglected such rotations by excluding the respective part of the kinetic energy. While this might be an appropriate approximation in HCN/CNH where H does not influence significantly the overall inertia tensor of the bent configurations, it becomes more problematic in LiNC/NCLi because Li is heavier and moves at larger distances. The complete rotation–vibration system requires, therefore, further study.

Acknowledgements

This work was made possible by the CNRS research position granted to D.S. for the 6 months in 2003. D.S. and J.T. acknowledge support by the EU network project Mechanics and Symmetry in Europe (MASIE), contract no. HPRN-CT-2000-00113.

References

- [1] R.H. Cushman, J.J. Duistermaat, Bull. Am. Math. Soc. 19 (1988) 475.
- [2] S. Vũ Ngọc, Commun. Math. Phys. 203 (1999) 465.
- [3] R.H. Cushman, L. Bates, Global Aspects of Classical Integrable Systems, Birkhauser, Basel, 1997.
- [4] D.A. Sadovskii, R.H. Cushman, Physica D 142 (2000) 166.
- [5] I.N. Kozin, R.M. Roberts, J. Chem. Phys. 118 (2003) 10523.
- [6] M.S. Child, T. Weston, J. Tennyson, Mol. Phys. 96 (1999) 371.
- [7] D.A. Sadovskii, B.I. Zhilinskií, Phys. Lett. A 256 (1999) 235.
- [8] H. Waalkens, A. Junge, H.R. Dullin, J. Phys. A. Math. Gen. 36 (2003) L307.
- [9] M.P. Jacobson, M.S. Child, J. Chem. Phys. 114 (2001) 262.
- [10] K. Efstathiou, M. Joyeux, D.A. Sadovskii, Phys. Rev. A (2003) (submitted).
- [11] D. Sugny, M. Joyeux, J. Chem. Phys. 112 (2000) 31.
- [12] D. Sugny, M. Joyeux, E.L. Sibert III, J. Chem. Phys. 113 (2000) 7165.
- [13] M. Joyeux, D. Sugny, Can. J. Phys. 80 (2002) 1459.
- [14] R. Essers, J. Tennyson, P.E.S. Wormer, Chem. Phys. Lett. 89 (1982) 223.
- [15] J.R. Henderson, J. Tennyson, Mol. Phys. 69 (1990) 639.
- [16] T. van Mourik, G.J. Harris, O.L. Polyansky, J. Tennyson, A.G. Császár, P.J. Knowles, J. Chem. Phys. 115 (2001) 3706.